Nucl. Phys. B 1020 (2025) 117141

Contents lists available at ScienceDirect

Nuclear Physics, Section B

journal homepage: www.elsevier.com/locate/nuclphysb

High Energy Physics - Theory

Existence of conformal symmetric wormhole with phantom energy in $f(R, L_m, T)$ theory

Doğukan Taşer

Çanakkale Onsekiz Mart University Department of Electricity and Energy, Çan Vocational School, Çanakkale, 17400, Türkiye

ARTICLE INFO

Editor name: John Charles

Keywords:
Conformal wormhole
$f(R, L_m, T)$ Theory
Killing vectors

ABSTRACT

In this study, we construct a traversable wormhole solution within the framework of $f(R, L_m, T)$ gravity by assuming conformal symmetry. The matter content is modeled using phantom energy, characterized by an equation of state parameter $\omega < -1$, which inherently violates the null energy condition. By employing conformal Killing vector symmetry, we derive exact analytical expressions for the shape function, energy density, and pressure components of the anisotropic fluid. Our analysis includes a detailed examination of the flare-out condition, proper radial distance, embedding diagrams, and the generalized Tolman-Oppenheimer-Volkoff equation. Notably, the model yields a positive active gravitational mass and positive total gravitational energy, despite the presence of exotic matter.

1. Introduction

Symmetries form the backbone of modern theoretical physics, providing a foundational language through which the laws of nature are formulated and understood. From classical mechanics to quantum field theory, symmetry principles help simplify complex systems, dictate conservation laws, and often point toward deeper physical truths. Among the various types of symmetry, such as translational, rotational, and gauge symmetries, conformal symmetry holds a special place, particularly in theories involving spacetime structure and gravitation.

Conformal symmetry refers to the invariance of the spacetime metric under local rescalings:

$$g_{ij} \to \Omega^2(x) g_{ij}, \tag{1}$$

where $\Omega(x)$ is a smooth, non-zero scalar function of the space-time coordinates [1,2]. Unlike isometries that preserve distances, conformal transformations preserve angles and the causal structure. A space-time admits conformal symmetry if it possesses a vector field ξ^i, known as a conformal Killing vector (CKV), satisfying the conformal Killing equation:

$$\mathcal{L}_\eta g_{ij} = \psi(x) g_{ij}, \tag{2}$$

where $\mathcal{L}_\eta$ denotes the Lie derivative along η^i, and $\psi(x)$ is the conformal factor [1,2]. The existence of such symmetries can greatly constrain the form of the metric and energy-momentum tensor, facilitating the construction of exact solutions in gravitational theories, especially when investigating exotic geometries such as wormholes.

Wormholes are hypothetical topological structures that act as bridges connecting separate points in spacetime. First proposed as solutions within general relativity (GR) [3], wormholes have attracted attention due to their implications for causality [4], quantum gravity [5], and interstellar travel [6]. A wormhole is said to be traversable if it allows for matter or signals to pass through from

E-mail address: dogukantaser@comu.edu.tr

https://doi.org/10.1016/j.nuclphysb.2025.117141
Received 2 August 2025; Received in revised form 8 September 2025; Accepted 22 September 2025
Available online 25 September 2025

one mouth to another without encountering event horizons or curvature singularities [3]. However, within the framework of GR, traversability typically requires the violation of the null energy condition (NEC), which states that $T_{ij}k^ik^j \geq 0$ for all null vectors k^i. This violation implies the necessity of exotic matter, raising questions about the physical realizability of such structures. arious methods have been investigated by researchers to construct wormhole geometries, either through the inclusion of standard matter or by minimizing the requirement for exotic components [7–10]. Furthermore, studies conducted on different alternative gravity theories have shown that wormhole geometry is possible without the need for exotic matter [11–15].

Conformal wormhole solutions constructed under the assumption that spacetime admits conformal symmetry have attracted considerable attention in recent years. These configurations not only aim to preserve the geometric and causal viability of traversable wormholes but also exploit symmetry induced constraints to simplify and regularize the underlying field equations. In this context, it is a well established approach to consider inheritance symmetry, which facilitates a natural correspondence between the spacetime geometry and the matter-energy distribution of the astrophysical system being modeled. In the quest to construct physically viable wormholes in modified theories of gravity, conformal symmetry has emerged as a powerful mathematical and physical tool. Taser et al. [16] constructed conformally symmetric wormhole solutions in $f(R, L_m)$ gravity and analyzed the physical significance of the supporting matter sources using a volume quantifier. Banerjee et al. [17] explored wormholes in $f(R, T)$ gravity using CKVs and showed that the NEC can be minimally violated in spatially restricted regions. Traversable phantom wormhole solutions in $f(R, \phi, \chi)$ gravity have been constructed by Wu [18], employing conformal symmetry and a linear equation of state, demonstrating their physical viability and stability. Jan et al. [19] investigated traversable wormhole solutions in the framework of $f(Q)$ gravity by employing conformal symmetry, and analyzed the violation of energy conditions indicating the presence of exotic matter. Likewise, Tayde et al. [20] considered noncommutative geometries within $f(Q, T)$ gravity and found that conformal symmetry allows for the construction of geometrically consistent wormholes while preserving the physical plausibility of the matter sector.

The late-time accelerated expansion of the universe presents a major challenge for GR on cosmological scales, unless one incorporates an additional component like dark energy [21,22]. This has motivated the exploration of modified gravity theories, which generalize the Einstein-Hilbert action to include additional curvature invariants and non-minimal couplings between matter and geometry [23,24]. One such model is the $f(R, L_m, T)$ gravity, where the action depends on the Ricci scalar R, the matter Lagrangian L_m, and the trace of the energy-momentum tensor T [25]. This theory introduces a direct coupling between matter and geometry, allowing for a richer phenomenology, but also leading to challenges such as non-conservation of the energy-momentum tensor and deviations from geodesic motion [25,26]. In recent years, the $f(R, L_m, T)$ gravity has garnered increasing attention. Mishra et al. [27] introduced the cosmographic treatment of this theory, employing observational datasets to constrain its parameters and demonstrating its viability in explaining late-time cosmic acceleration. Zubair et al. [28] further extended this approach by incorporating thermodynamical laws and perturbative stability analysis, concluding that several reconstructed models satisfy generalized second law of thermodynamics and remain stable by small perturbations. Arora et al. [29] focused on the energy conditions in $f(R, L_m, T)$ gravity, deriving constraints on model parameters and showing that viable ranges can be found without invoking exotic matter. Maurya [30] constructed five distinct cosmological models under flat FLRW spacetime and demonstrated that several of them exhibit transit-phase acceleration compatible with ΛCDM predictions. Gonçalves and Santos [31] explored the causality structure of $f(R, L_m, T)$ gravity through Gödel-type metrics, revealing that the theory allows both causal and non-causal solutions depending on the matter content and parameter constraints, and introducing a critical radius demarcating causality violation.

The study of traversable wormholes under $f(R, L_m, T)$ gravity has emerged as an active research area, motivated by the theory's capability to suppress or eliminate the necessity of exotic matter. Moraes et al. [32] constructed wormhole in a linear $f(R, L_m, T)$ model. These configurations satisfy the geometric traversability criteria while allowing for ordinary matter sources. Errehymy et al. [33] introduced Einstein cluster models into this framework, illustrating how tangential pressure-dominated fluids resembling dark matter halos can generate stable wormholes that align with observed lensing phenomena. Naseer et al. [34] emphasized the role of different equations of state and gravitational complexity in shaping viable wormhole geometries, demonstrating that $f(R, L_m, T)$ gravity permits NEC-violating configurations without violating physical stability. Tayde and Sahoo [35] examined the effect of the Equation of State (EoS) parameters on lensing and matter content, confirming that certain parameter choices allow for repulsive gravitational behavior and positive active mass. Furthermore, Tayde et al. [36] explored wormhole geometries with strange quark matter using the MIT bag model and confirmed that, despite NEC violation, the resulting wormholes remain physically stable and exhibit a gravitational field similar to that of ordinary matter. By employing CKVs, we aim to systematically constrain the geometry-matter interaction and derive exact wormhole configurations that are not only traversable and stable but also minimize exotic matter requirements. Our approach highlights the geometric richness introduced by conformal symmetry and reinforces upside of $f(R, L_m, T)$ gravity to a fertile ground for realistic wormhole models.

The structure of this paper is organized: In Section 2, we present the general formalism of $f(R, L_m, T)$ gravity and outline the specific linear form of the model employed in this work. Section 3 introduces the Morris-Thorne wormhole geometry in $f(R, L_m, T)$ and derives the corresponding field equations for an anisotropic fluid source. In Section 4, we impose CKVs to obtain exact solutions for the metric functions and matter content, and analyze the physical and geometric properties of the wormhole configuration. Finally, the main results and their implications are summarized in Section 5.

2. $f(R, L_m, T)$ gravity

The action for the $f(R, L_m, T)$ gravity is described as [25,26]:

$$I = \int d^4x \sqrt{-g}\Big[\frac{1}{16\pi} f(R, L_m, T) + L_m\Big] \tag{3}$$

This generalized action includes a coupling between the geometry (via R), the matter Lagrangian density L_m, and the trace T of the energy-momentum tensor. Variation of Eq. (3) provides:

$$\delta I = \frac{1}{16\pi}\int d^4x\,\sqrt{-g}\left[f_R\delta R + (f_T\frac{\delta T}{\delta g^{ij}} + f_{L_m}\frac{\delta L_m}{\delta g^{ij}} - \frac{1}{2}g_{ij}f - 8\pi T_{ij}\delta g^{ij}\right] \tag{4}$$

Here, partial derivatives of f are defined as $f_R = \partial f/\partial R$, $f_{L_m} = \partial f/\partial L_m$, and $f_T = \partial f/\partial T$ [25,26]. The field equations for theory are attained:

$$f_R R_{ij} - \frac{1}{2}\left[f(R,L_m,T) - (f_{L_m} + 2f_T)L_m\right]g_{ij} + (g_{ij}\Box - \nabla_i\nabla_j)f_R = \left[8\pi + \frac{1}{2}(f_{L_m} + 2f_T)\right]T_{ij} + f_T\tau_{ij} \tag{5}$$

The field equations contain additional source terms, which reflect the non-minimal coupling between matter and geometry [25,26]. The energy-momentum tensor is identified as:

$$T_{ij} = -\frac{2}{\sqrt{-g}}\frac{\delta(\sqrt{-g}L_m)}{\delta g^{ij}} \tag{6}$$

This standard expression relates the variation of L_m to the energy-momentum tensor. An auxiliary tensor appears due to second-order variations of the Lagrangian [25]:

$$\tau_{ij} \equiv 2g^{kl}\frac{\partial^2 L_m}{\partial g^{ij}\partial g^{kl}} \tag{7}$$

This term generally vanishes for simple matter sources like perfect fluids. Taking the covariant derivative of the field equations, one obtains:

$$\begin{aligned} &R_{ij}\nabla^i f_R + f_R\nabla^i R_{ij} - \frac{1}{2}\nabla_j f(R,L_m,T) = \left[8\pi + \frac{1}{2}(f_{L_m} + 2f_T)\right]\nabla^i T_{ij} \\ &+ (\Box\nabla_j - \nabla_j\Box)f_R - \nabla_j\left[\left(\frac{1}{2}f_{L_m} + f_T\right)L_m\right] + T_{ij}\nabla^i\left(\frac{1}{2}f_{L_m} + f_T\right) + \nabla^i(f_T\tau_{ij}) \end{aligned} \tag{8}$$

wehere $(\Box\nabla_j - \nabla_j\Box)f_R = R_{ij}\nabla^i f_R$. This relation shows that in theory, the energy-momentum tensor is generally not conserved. The modified conservation law is given by:

$$\nabla^i T_{ij} = \frac{1}{8\pi + f_m}\left[\nabla_j(L_m f_m) - T_{ij}\nabla^i f_m - \nabla^i(f_T\tau_{ij}) - \frac{1}{2}\left(f_T\nabla_j T + f_{L_m}\nabla_j L\right)\right] \tag{9}$$

Here, the quantity f_m is defined as $f_m = f_T + \frac{1}{2}f_{L_m}$ [37]. This expression reflects the non-conservation of the energy-momentum tensor due to the explicit geometry-matter coupling.

3. Morris-thorne wormhole in $f(R, L_m, T)$ gravity

We consider line element of wormhole spacetime as [3]:

$$ds^2 = e^{2\Phi(r)}dt^2 - \frac{dr^2}{1 - \frac{S(r)}{r}} - r^2(d\theta^2 + \sin^2\theta\, d\phi^2) \tag{10}$$

In this metric: - $\Phi(r)$ is known as the redshift function, which must be finite everywhere to avoid the formation of event horizons, - $S(r)$ is the shape function designating the spatial shape of the wormhole and must satisfy specific conditions at the throat.

The wormhole throat is located at the minimum radius $r = r_0$, where $S(r_0) = r_0$. For the wormhole to be traversable, the following conditions must be achieved: (i) At the throat, the derivative of the shape function must hold $S'(r_0) < 1$ to ensure the geometry flares outward. (ii) To allow for traversability, $\Phi(r)$ must be finite for all r, avoiding the presence of horizons that would prevent two-way travel. (iii) For $r \to \infty$, both $\Phi(r) \to 0$ and $S(r)/r \to 0$, so that the spacetime becomes Minkowskian at spatial infinity [3].

Also, an anisotropic fluid is considered as the energy momentum tensor whose components are defined as follows

$$T^i_j = diag[p_r, p_t, p_t, -\rho] \tag{11}$$

where ρ is the energy density, p_t is the tangential pressure and p_r is the radial pressure [3,38].

$f(R, L_m, T)$ function is considered as follows:

$$f(R, L_m, T) = \frac{R}{2} + \alpha L_m + \beta T, \tag{12}$$

where α and β are constants that parameterize the strength of the gravitational and matter coupling terms, respectively. Beyond its formal simplicity, the model $f(R, L_m, T) = \frac{R}{2} + \alpha L_m + \beta T$ and assuming $L_m = -\rho$ proves particularly advantageous in applications to compact objects and cosmology [25,35,39]. By considering Eqs. (5), (10)–(12), one get field equations for Morris-Thorne wormhole with anisotropic fluid for linear $f(R, L_m, T)$ gravity:

$$-\frac{2\Phi' S}{r^2} + \frac{2\Phi'}{r} - \frac{S}{r^3} = \left(\lambda + \frac{\beta}{2}\right)p_r + \frac{\beta}{2}(2p_t + \rho) \tag{13}$$

$$
\begin{aligned}
&-\frac{\Phi'^2 S}{r}+\Phi'^2-\frac{\Phi' S'}{2r}-\frac{\Phi'' S}{r}+\Phi''-\frac{\Phi' S}{2r^2}+\frac{\Phi'}{r}-\frac{S'}{2r^2}+\frac{S}{2r^3}\\
&=(\lambda+\beta)p_t+\frac{\beta}{2}\left(p_r+\rho\right)
\end{aligned}
\tag{14}
$$

$$
\frac{S'}{r^2}=\left(\lambda-\frac{\beta}{2}\right)\rho-\frac{\beta}{2}\left(2p_t+p_r\right)
\tag{15}
$$

where λ is described as $\lambda = 8\pi + \frac{\alpha}{2} + \beta$. Despite constructing the field equations for Morris-Thorne type wormhole geometries in $f(R, L_m, T)$ gravity, obtaining exact analytical solutions proves to be extremely challenging due to the high degree of nonlinearity and coupling among the geometric and matter terms. The complexity of the resulting differential system prevents straightforward integration or simplification using conventional methods.

4. Conformal wormhole in $f(R, L_m, T)$ gravity

We investigate a wormhole spacetime that possesses conformal symmetry, characterized by the following conformal Killing equation:

$$
\mathcal{L}_\eta g_{ij}=g_{ni}\eta^n_{;j}+g_{in}\eta^n_{;j}=\psi(r)g_{ij}
\tag{16}
$$

Here, $\mathcal{L}_\eta$ denotes the Lie derivative of the metric tensor g_{ij} along the vector field η^i, and $\psi(r)$ is the conformal factor [40,41]. Assuming that the only non-vanishing component of the vector field is radial, i.e., $\eta^i = (\eta^1(r), 0, 0, 0)$, the conformal Killing condition applied to Eq. (10):

$$
\eta^1\Phi'(r)=\frac{\psi(r)}{2}
\tag{17}
$$

$$
\eta^1=\frac{r\psi(r)}{2}
\tag{18}
$$

$$
\eta^1\left(-\frac{S(r)-rS'(r)}{r^2-rS(r)}\right)+2\frac{d\eta^1}{dr}=\psi(r)
\tag{19}
$$

This equations constrains the form of $S(r)$ in terms of $\psi(r)$. Solving the system leads to explicit forms for the metric components [40–42]:

$$
e^{2\Phi(r)}=k_1^2r^2,\quad \left(1-\frac{S(r)}{r}\right)^{-1}=\frac{k_2^2}{\psi^2(r)}
\tag{20}
$$

Therefore, $S(r)$ can be reattained as:

$$
S(r)=r\left(1-\frac{\psi^2(r)}{k_2^2}\right)
\tag{21}
$$

These results show that the presence of conformal symmetry imposes a strong constraint on the wormhole geometry. Both the redshift and shape functions become explicitly dependent on $\psi(r)$, letting a unified treatment of space-time geometry based on symmetry principles. By considering Eqs. (20)-(21) in (13)–(15), one get field equations for conformal wormhole with anisotropic fluid for $f(R, L_m, T)$ gravity as follows:

$$
\frac{1}{r^2}\left(\frac{3\psi^2}{k_2^2}-1\right)=\left(\lambda+\frac{\beta}{2}\right)p_r+\frac{\beta}{2}\left(2p_t+\rho\right)
\tag{22}
$$

$$
\frac{\psi}{k_2^2 r}\left(2\psi'+\frac{\psi}{r}\right)=(\lambda+\beta)p_t+\frac{\beta}{2}\left(p_r+\rho\right)
\tag{23}
$$

$$
\frac{1}{r^2}-\frac{\psi}{k_2^2 r}\left(2\psi'+\frac{\psi}{r}\right)=\left(\lambda-\frac{\beta}{2}\right)\rho-\frac{\beta}{2}\left(2p_t+p_r\right)
\tag{24}
$$

In order to get a valid solution, we consider linear equation of state (EoS) described a relation between energy density and radial pressure [42]:

$$
p_r=\omega\rho
\tag{25}
$$

Under the assumption of EoS, all unknown quantities for conformal wormhole in linear $f(R, L_m, T)$ gravity are attained as follows:

$$
\psi(r)^2=k_3\, r^{\frac{(2\omega-2)\beta-2\lambda(\omega+3)}{(\omega-1)\beta+2\lambda\omega}}+\frac{k_2^2(\omega+1)(\lambda+\beta)}{(1-\omega)\beta+\lambda(\omega+3)}
\tag{26}
$$

$$\rho(r) = \frac{6k_3\, r^{\frac{-6\lambda(\omega+1)}{(2\lambda+\beta)\omega-\beta}}}{k_2^2[(\omega-1)\beta+2\lambda\omega]} + \frac{2(\lambda+\beta)}{[\lambda(\omega+3)-(\omega-1)\beta]\lambda\, r^2} \tag{27}$$

$$p_r(r) = \frac{6\omega k_3\, r^{\frac{-6\lambda(\omega+1)}{(2\lambda+\beta)\omega-\beta}}}{k_2^2[(\omega-1)\beta+2\lambda\omega]} + \frac{2\omega(\lambda+\beta)}{[\lambda(\omega+3)-(\omega-1)\beta]\lambda\, r^2} \tag{28}$$

$$p_t(r) = \frac{-6k_3\, r^{\frac{-6\lambda(\omega+1)}{(2\lambda+\beta)\omega-\beta}}}{k_2^2[(\omega-1)\beta+2\lambda\omega]} + \frac{(\lambda-\beta)(\omega+1)}{[\lambda(\omega+3)-(\omega-1)\beta]\lambda\, r^2} \tag{29}$$

In order to get shape function by considering Eq. (26) in (21), one gets

$$S(r) = -\frac{k_3}{k_2^2} r^{\frac{(3\omega-3)\beta-6\lambda}{(\omega-1)\beta+2\lambda\omega}} + \frac{2r(\lambda-\omega\beta)}{(\lambda-\beta)\omega+3\lambda+\beta} \tag{30}$$

For an asymptotically flat wormhole, both the redshift function and the $S(r)/r$ function should approach zero as $r \to \infty$. From Eq. (20), redshift function is obtained as $\Phi(r) = \ln(k_1 r)$. Conformal symmetry is known to break the asymptotic flatness of wormhole geometries, as the redshift function fails to vanish in the limit $r \to \infty$. Therefore, the spacetime must be cut off at a certain radial point $r = r_1$ and joined continuously to an exterior vacuum region. By considering matching conditions, unknown constant, k_1, is obtained as

$$k_1 = \frac{e^{\Phi(r_1)}}{r_1}. \tag{31}$$

Hence, the redshift function becomes:

$$\Phi(r) = \ln\left(\frac{r e^{\Phi(r_1)}}{r_1}\right) \tag{32}$$

In addition, when this condition is analysed depending on the shape function, the function $S(r)/r$ becomes constant as $r \to \infty$. If the second term in $S(r)$ given by Eq. (30) is zero, $S(r)/r$ becomes zero in the case of $\frac{3\beta}{2\lambda-\beta} > 0$. For this reason, the EoS parameter is chosen as $\omega = \frac{\lambda}{\beta}$ in the case of $\omega < -1$. The matter regime corresponds to phantom energy. It is clear that the selection of the matter as a phantom energy accordingly the constants in the $f(R, L_m, T)$ function. Here, the selection of the constants α, β and, consequently, λ is arranged in the remainder of the study to correspond to the phantom energy. In this case all quantities are

$$S(r) = -\frac{k_3}{k_2^2} r^{-\frac{3\beta}{2\lambda-\beta}} \tag{33}$$

$$\rho(r) = \frac{\left(3r^{\frac{-2(\lambda+\beta)}{2\lambda-\beta}} k_3\lambda + (2\lambda-\beta)k_2^2\right)\beta}{r^2\left(\lambda-\frac{\beta}{2}\right)\lambda k_2^2(\lambda+\beta)} \tag{34}$$

$$p_r(r) = \frac{\left(6r^{\frac{-2(\lambda+\beta)}{2\lambda-\beta}} k_3 + 4k_2^2\right)\lambda - 2k_2^2\beta}{(\lambda+\beta)(2\lambda-\beta)\, r^2\, k_2^2} \tag{35}$$

$$p_t(r) = \frac{2k_2^2\lambda^2 - \left(6r^{\frac{-2(\lambda+\beta)}{2\lambda-\beta}} k_3 + 3k_2^2\right)\beta\lambda + k_2^2\beta^2}{(\lambda+\beta)(2\lambda-\beta)\, r^2\, k_2^2\, \lambda} \tag{36}$$

Attention is now directed toward assessing whether the obtained shape function $S(r)$ fulfills the physical criteria necessary for the existence of a traversable wormhole. In Eq. (33),the throat condition, $S(r_0) = r_0$, yields the relation

$$-\frac{k_3}{k_2^2} r_0^{-\frac{3\beta}{2\lambda-\beta}} = r_0 \quad \Rightarrow \quad r_0^{1+\frac{3\beta}{2\lambda-\beta}} = -\frac{k_3}{k_2^2}, \tag{37}$$

which determines the throat radius r_0 in terms of the model parameters. The flaring-out condition, $S'(r_0) < 1$, requires the derivative

$$S'(r) = \frac{3\beta k_3}{k_2^2(2\lambda-\beta)} r^{-\left(\frac{3\beta}{2\lambda-\beta}+1\right)} \tag{38}$$

to satisfy

$$S'(r_0) = \frac{3\beta k_3}{k_2^2(2\lambda-\beta)} r_0^{-\left(\frac{3\beta}{2\lambda-\beta}+1\right)} < 1, \tag{39}$$

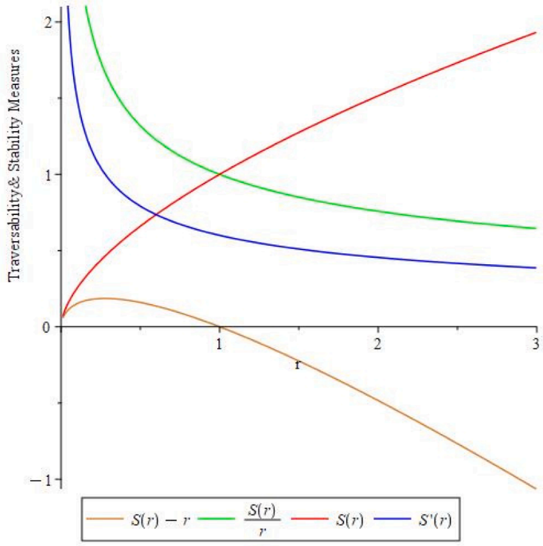

Fig. 1. (i) $S(r) - r$ function (brown line) (ii) $S(r)/r$ function (green line) (iii) $S(r)$ function (red line) (iv) $S'(r)$ function (blue line) with a throat radius of $r_0 = 1$ with $k_2 = 1$, $k_3 = -1$, $\alpha = -13\pi$ and $\beta = -\pi/2$. (For interpretation of the references to colour in this figure legend, the reader is referred to the web version of this article.)

which imposes constraints on the parameters β, λ, and the constants k_2, k_3. Additionally, the metric condition $S(r) \leq r$ for all $r \geq r_0$ translates into

$$-\frac{k_3}{k_2^2} r^{-\frac{3\beta}{2\lambda-\beta}} \leq r \quad \Rightarrow \quad -\frac{k_3}{k_2^2} \leq r^{1+\frac{3\beta}{2\lambda-\beta}}, \tag{40}$$

which is naturally satisfied for $r \geq r_0$, provided that $S(r)$ is monotonically decreasing. Therefore, under the conditions $k_3 < 0$ and $-\frac{3\beta}{2\lambda-\beta} < 1$, the function $S(r)$ holds all the geometric criteria required for a viable traversable wormhole solution. In order to analyse the viable traversable wormhole solution with respect to the preference of constants in $f(R, L_m, T)$ function, acceptable value ranges of α and β in the case of $k_3 < 0$ are defined as follows

$$\alpha \in \begin{cases} (-\infty, -(4\beta + 16\pi)) \cup \big(-(\beta + 16\pi), \infty\big), & \text{if } \beta > 0, \\ (-\infty, -(\beta + 16\pi)) \cup \big(-(4\beta + 16\pi), \infty\big), & \text{if } \beta < 0, \\ \mathbb{R} \setminus \{-16\pi\}, & \text{if } \beta = 0. \end{cases}$$

The shape function and the changes of the functions associated with the related traversability conditions are illesturated in Fig. 1. The condition $S(r)/r < 1$ near the throat confirms the flare-out requirement for traversable wormholes, while the derivative profile $S'(r)$ supports geometric regularity. The wormhole throat is located at the radial coordinate where the expression $S(r) - r$ intersects the r-axis. Furthermore, although the redshift function does not vanish in the limit $r \to \infty$, the quantity $\frac{S(r)}{r}$ asymptotically approaches zero. This behavior indicates that the spacetime is not asymptotically flat due to the structure of the redshift function. As shown in Fig. 1, the derivative of the shape function at the throat satisfies the condition $S'(r_0) < 1$, thereby ensuring that the flaring-out condition is met.

4.1. Embedding surface

To enhance our understanding of the wormhole geometry defined by Eq. (33), we present its spatial shape through two-dimensional and three-dimensional embedding diagrams based on $S(r)$. Since the spacetime under consideration is spherically symmetric, we simplify our analysis by choosing an equatorial slice where $\theta = \pi/2$, and by fixing the time coordinate t to be constant. On this hypersurface, where $d\theta = 0$ and $dt = 0$, the wormhole metric simplifies to:

$$ds^2 = -\frac{dr^2}{1 - \frac{S(r)}{r}} - r^2 d\phi^2. \tag{41}$$

In cylindrical coordinates, the line element on a flat three-dimensional Euclidean space is expressed as:

$$ds^2 = -dz^2 - dr^2 - r^2 d\phi^2. \tag{42}$$

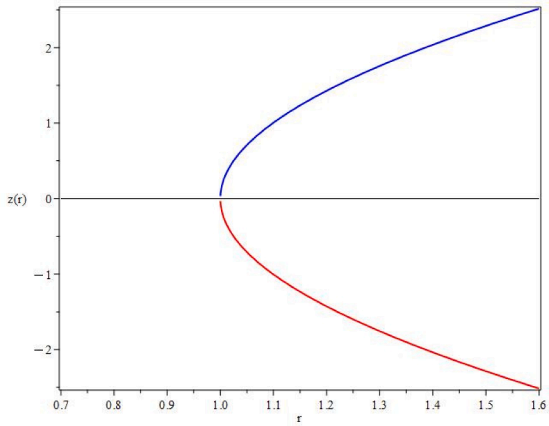

Fig. 2. 2D Embedding diagram for conformal wormhole ($k_2 = 1, k_3 = -1, \beta = -\frac{\pi}{2}, \lambda = \pi$ and $r_0 = 1$).

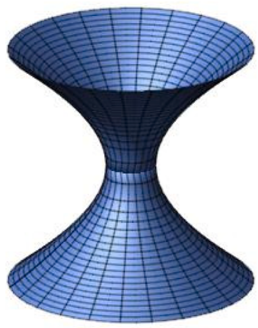

Fig. 3. 3D Embedding diagram for conformal wormhole ($k_2 = 1, k_3 = -1, \beta = -\frac{\pi}{2}, \lambda = \pi$ and $r_0 = 1$).

Assuming the embedding surface takes the form $z = z(r)$, the metric becomes:

$$ds^2 = -\left[1 + \left(\frac{dz}{dr}\right)^2\right] dr^2 - r^2 d\phi^2. \tag{43}$$

By comparing the two expressions above, we obtain the embedding profile, $z(r)$, as:

$$\frac{dz}{dr} = \pm\sqrt{\left(1 - \frac{S(r)}{r}\right)^{-1} - 1}. \tag{44}$$

This expression allows us to generate the embedding diagrams used to visualize the wormhole's spatial shape [43]. By considering Eqs. (33) and (41)–(44), the 2D and 3D embedding diagram for conformal wormhole is illustrated in Figs. 2 and 3. The diagrams illustrate the throat structure and global geometry of the spacetime, highlighting its regularity and the flare-out condition necessary for traversability.

4.2. Proper radial distance

To investigate the radial profile of the wormhole more effectively, we adopt a proper radial coordinate system. Within this framework, the metric is expressed as:

$$ds^2 = e^{2\Phi(l)} dt^2 - dl^2 - r(l)^2 \left(d\theta^2 + \sin^2\theta\, d\phi^2\right), \tag{45}$$

where $l(r)$ represents the proper distance measured from the wormhole's throat [44,45]. This quantity can be determined by integrating over the radial coordinate as follows:

$$l(r) = \pm \int_{r_0}^{r} \left(1 - \frac{S(r)}{r}\right)^{-1/2} dr, \tag{46}$$

where the plus and minus signs correspond to the two asymptotically flat regions on either side of the wormhole throat at $r = r_0$. The integral above reflects how proper spatial lengths differ from coordinate distances in the vicinity of the throat. It should be emphasized that the proper radial distance l always satisfies the condition $|l(r)| \geq r - r_0$ which means that the actual physical distance through the

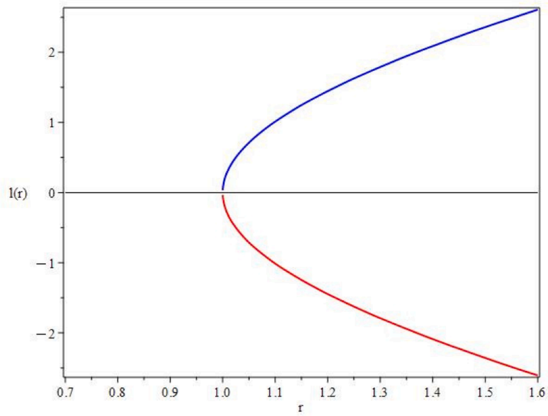

Fig. 4. Proper distance for conformal wormhole ($k_2 = 1, k_3 = -1, \beta = -\frac{\pi}{2}, \lambda = \pi$ and $r_0 = 1$).

wormhole exceeds or equals the simple coordinate difference. This distance decreases continuously from $+\infty$ to 0 as one approaches the throat from one universe, and symmetrically increases from 0 to $-\infty$ on the opposite side [44,45]. By considering Eqs. (33) and (46), the proper distance for conformal wormhole is illustrated in Fig. 4. In Fig. 4, the proper distance adapts to condition of $|l(r)| \geq r - r_0$. The function $l(r)$ attains a minimum at the throat and grows symmetrically on both sides, supporting the traversability and regularity of the wormhole geometry. As a result of the numerical analysis performed, it was found that the $l(r)$ function is greater than the $z(r)$ function for the conformal wormhole.

4.3. Energy conditions

The Raychaudhuri equations are fundamental in general relativity, governing the evolution of congruences of geodesics and providing critical insight into the focusing behavior of geodesic flows. These equations directly connect to the classical energy conditions the weak, strong, dominant, and null energy conditions which impose constraints on the energy-momentum tensor to provide physically reasonable matter content [46]. The violation of these energy conditions, particularly the null and weak energy conditions, becomes unavoidable to satisfy the flare-out condition at the throat, which guarantees the traversability of the geometry for a wormhole model [19]. Therefore, the energy conditions is essential to assess the physical viability and theoretical consistency of proposed wormhole geometries.

Weak Energy Condition (WEC)

$$T_{ij}u^i u^j \geq 0 \quad \Rightarrow \quad \rho \geq 0, \quad \rho + p_r \geq 0, \quad \rho + p_t \geq 0 \tag{47}$$

Null Energy Condition (NEC)

$$T_{ij}\sigma^i \sigma^j \geq 0 \quad \Rightarrow \quad \rho + p_r \geq 0, \quad \rho + p_t \geq 0 \tag{48}$$

where σ^i is a null vector satisfying $\sigma^i \sigma_k = 0$.

Strong Energy Condition (SEC)

$$\left(T_{ij} - \frac{1}{2}T g_{ij}\right)u^i u^j \geq 0 \quad \Rightarrow \quad \rho + p_r + 2p_t \geq 0 \tag{49}$$

Dominant Energy Condition (DEC)

$$\begin{aligned} T_{ij}u^i u^j \geq 0, \quad T_{ij}u^i \text{ is non-spacelike} \quad \Rightarrow \quad & \rho - |p_r| \geq 0, \\ & \rho - |p_t| \geq 0 \end{aligned} \tag{50}$$

By considering Eqs. (27)–(29), the functions related to energy conditions are attained as follows:

$$\rho(r) + p_r(r) = \frac{6r^{\frac{-2(\lambda+\beta)}{2\lambda-\beta}} k_3 \lambda + 2k_2^2(2\lambda - \beta)}{\lambda k_2^2 r^2 (2\lambda - \beta)} \tag{51}$$

$$\rho(r) + p_t(r) = \frac{1}{\lambda r^2} \tag{52}$$

$$\rho(r) - p_r(r) = -\frac{2(\lambda - \beta)\left(3r^{\frac{-2(\lambda+\beta)}{2\lambda-\beta}} k_3 \lambda + k_2^2(2\lambda - \beta)\right)}{(2\lambda - \beta) r^2 k_2^2 \lambda(\lambda + \beta)} \tag{53}$$

$$\rho(r) - p_t(r) = \frac{12r^{\frac{-2(\lambda+\beta)}{2\lambda-\beta}} k_3 \lambda\beta - k_2^2(2\lambda - \beta)(\lambda - 3\beta)}{(2\lambda - \beta) r^2 k_2^2 \lambda(\lambda + \beta)} \tag{54}$$

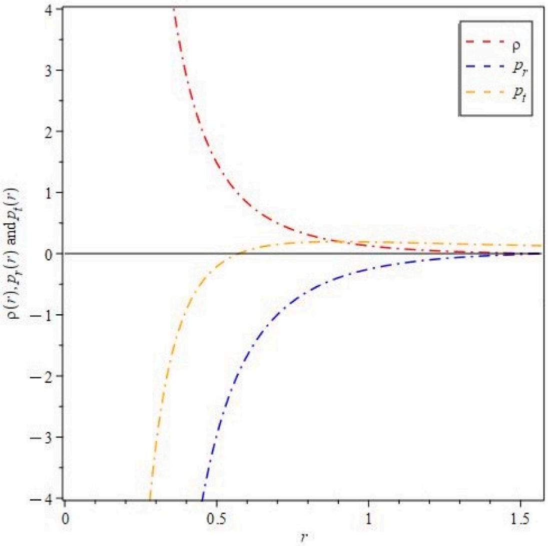

Fig. 5. The evolution of energy density, radial pressure and tangential pressure for conformal wormhole ($k_2 = 1, k_3 = -1, \beta = -\frac{\pi}{2}, \lambda = \pi$ and $r_0 = 1$).

$$\rho(r) + p_r(r) + 2p_t(r) = \frac{6k_3(\lambda-\beta)r^{\frac{-2(\lambda+\beta)}{2\lambda-\beta}} + 4k_2^2(2\lambda-\beta)}{(2\lambda-\beta)r^2k_2^2(\lambda+\beta)} \tag{55}$$

The energy conditions for the conformal wormhole were examined with the help of graphical representation. It is worth mentioning that the constants for the $f(R, L_m, T)$ function is selected as $\beta = -\frac{\pi}{2}$ and $\alpha = -13\pi$, respectively. In this case, when we consider the EoS, the matter distribution corresponds to phantom energy, where $\omega < -1$. To understand the structure of the matter distribution, the changes of matter components under fixed constants are presented in Fig. 5. In Fig. 5, it shows that when ρ is positive, p_r is negative, and both approach zero as the value of r increases. Also, it is observed that the tangential pressure function p_t becomes zero at a point smaller than the throat radius $r_0 = 1$, approximately around $r_* \approx 0.572$. This implies that the tangential pressure exhibits a negative character in the region $r_* < r_0$, while it turns positive for $r_* > r_0$. Such behavior of the anisotropic fluid in this region can be interpreted as a negative tangential tension contributing to the stability of the throat. The fact that this transition occurs inside the throat region is significant, as it supports the flare-out condition of the spacetime geometry.

The evolution of energy conditions is shown in Fig. 6. The curves represent the NEC, WEC, SEC, and DEC combinations. Near the throat, certain conditions are violated, however, these violations are localized, indicating a physically reasonable configuration. Despite the conditions $\rho > 0$ and $\rho + p_t > 0$ are hold for the conformal wormhole, WEC is not hold due to the condition $\rho + p_r < 0$. Also, NEC is not satisfied due to the condition $\rho + p_r < 0$. While $\rho - p_r$ is positive and it is approaches to zero, $\rho - p_t$ is positive and then it turns negative around throat of wormhole. It causes the DEC not to be met. SEC is not satisfied,as well. It is negative and turns positive around $r \approx 0.779$.

4.4. Generalized TOV equation

In GR, the Tolman-Oppenheimer-Volkoff (TOV) [47] equation describes the condition for hydrostatic equilibrium in matter distribution. For anisotropic matter, the TOV equation is described as [48]:

$$\frac{\varpi'}{2}(\rho + p_r) + \frac{dp_r}{dr} + \frac{2}{r}(p_r - p_t) = 0, \tag{56}$$

where ϖ is related to the redshift function ($\varpi = 2\Phi(r)$). This equation can be decomposed into three distinct force components: $F_h = -\frac{dp_r}{dr}$, $F_g = -\frac{\varpi'}{2}(\rho + p_r)$ and $F_a = \frac{2}{r}(p_t - p_r)$ represent the hydrostatic, gravitational, and anisotropic forces. By considering Eqs. (34)–(36), distinct force components are obtained as follows

$$F_h = \frac{36\,r^{\frac{-2(\lambda+\beta)}{2\lambda-\beta}}\,k_3\,\lambda^2 + 16\left(\lambda - \frac{\beta}{2}\right)^2 k_2^2}{(2\lambda-\beta)^2\,r^3\,k_2^2\,(\lambda+\beta)} \tag{57}$$

$$F_g = \frac{-6\,r^{\frac{-2(\lambda+\beta)}{2\lambda-\beta}}\,k_3\,\lambda - 4\,k_2^2\left(\lambda - \frac{\beta}{2}\right)}{(2\lambda-\beta)\,r^3\,k_2^2\,\lambda} \tag{58}$$

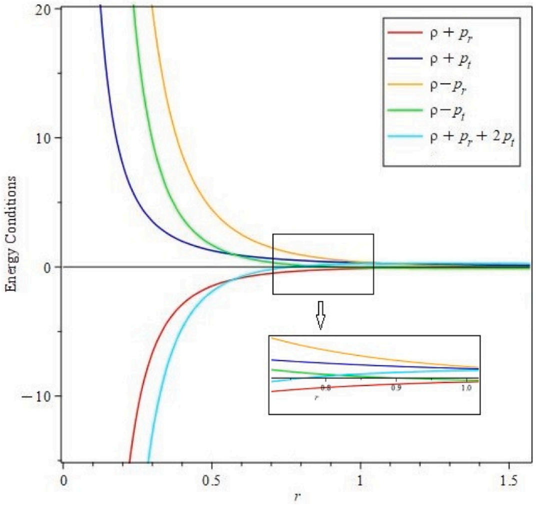

Fig. 6. The evolution of energy conditions for conformal wormhole ($k_2 = 1, k_3 = -1, \beta = -\frac{\pi}{2}, \lambda = \pi$ and $r_0 = 1$).

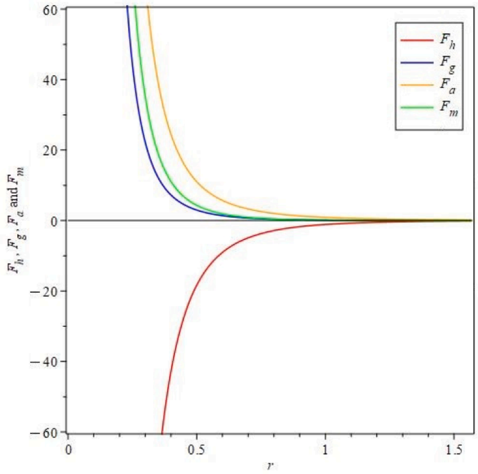

Fig. 7. The evolution of F_h,F_g, F_a and F_m for conformal wormhole ($k_2 = 1, k_3 = -1, \beta = -\frac{\pi}{2}, \lambda = \pi$ and $r_0 = 1$).

$$F_a = \frac{-12\, r^{\frac{-2(\lambda+\beta)}{2\lambda-\beta}}\, k_3\, \lambda - 4\, k_2^2 \left(\lambda - \frac{\beta}{2}\right)}{(2\lambda-\beta)\, r^3\, k_2^2\, \lambda} \tag{59}$$

Within the context of $f(R, L_m, T)$ gravity, the energy-momentum tensor is not conserved in the standard form, introducing additional effective force terms into the equilibrium condition. For $f(R, L_m, T) = R + \alpha L_m + \beta T$, it is attained as

$$-\frac{dp_r}{dr} - \frac{\varpi'}{2}(\rho + p_r) + \frac{2}{r}(p_t - p_r) - \frac{\beta}{2\lambda}(\rho' + p_r' + 2p_t') = 0 \tag{60}$$

where last term represents an additional effective force, F_m. By considering Eqs. (34)–(36), F_m is attained as

$$F_m = \frac{18\beta\left(k_3\, \lambda\, (\lambda-\beta)\, r^{\frac{-2\lambda-2\beta}{2\lambda-\beta}} + \frac{8}{9}\left(\lambda - \frac{\beta}{2}\right)^2 k_2^2\right)}{\lambda\, (2\lambda-\beta)^2\, r^3\, k_2^2\, (\lambda+\beta)} \tag{61}$$

In our conformal wormhole model, all force terms are found to be in balance, such that the generalized TOV equation is identically satisfied:

$$F_h + F_g + F_a + F_m = 0. \tag{62}$$

The evolution of all forces is illustrated in Fig. 7. This indicates that the system achieves hydrostatic equilibrium under the joint effect of anisotropic pressures and matter-geometry coupling, even in a phantom energy component marked by $\rho + p_r < 0$. These exotic properties indicate in the TOV dynamics, particularly making the hydrostatic force F_h negative and dominant. On the other hand, the remaining force terms are positive, playing a stabilizing role in the wormhole configuration. All four forces exhibit strong magnitudes near the throat (small r), and asymptotically decay to zero as r increases. This behavior emphasizes that static equilibrium in the phantom energy supported wormhole geometry is achieved through a delicate balance among the four interacting force components.

4.5. Volume integral quantifier

In order to assess the total amount of exotic matter necessary to sustain a traversable Lorentzian wormhole, one can utilize what is referred to as the volume integral quantifier. Originally definied by Visser et al. [49], this tool offers a way to estimate the averaged violation of the null energy condition within a finite region of spacetime. The integral is identified by

$$I_V = \int (\rho(r) + p_r(r))\, dV, \tag{63}$$

here the integration is performed over the spatial volume element $dV = r^2 \sin\theta\, dr\, d\theta\, d\phi$. Assuming that the matter distribution is cut off at a finite radius $r = a$, the integral can be rewritten in the form [50]:

$$\begin{aligned} I_V &= \left[r\left(1 - \frac{S}{r}\right) \ln\left(\frac{e^{2\Phi}}{1 - S/r}\right)\right]_{r_0}^{a} - \int_{r_0}^{a} (1 - S') \left[\ln\left(\frac{e^{2\Phi}}{1 - S/r}\right)\right] dr \\ &= \int_{r_0}^{a} (r - S) \left[\ln\left(\frac{e^{2\Phi}}{1 - S/r}\right)\right]' dr, \end{aligned} \tag{64}$$

where boundary term at the throat $r = r_0$ vanishes since $S(r_0) = r_0$ by construction. Using the specific form of the redshift function $e^{2\Phi(r)} = k_1^2 r^2$ and the previously derived expressions for the shape function $S(r)$, the volume integral for conformal wormhole becomes:

$$I_V = \left[2r - \frac{2\lambda\, k_3\, r^{-\frac{3\beta}{2\lambda - \beta}}}{k_2^2 \beta} \right]_{r_0}^{a}. \tag{65}$$

Taking the limit $a \to r_0$, it follows that $I_V \to 0$. This result implies, consistent with the findings in Lobo [51,52], that it is theoretically possible to construct conformal symmetric phantom wormholes supported by an arbitrarily small quantity of phantom energy, which minimally violates the averaged null energy condition.

4.6. Active gravitational mass of wormholes

The notion of a wormhole's active gravitational mass is essential for understanding how such geometries gravitate and interact with the surrounding spacetime. Remarkably, even though wormholes are typically sustained by exotic matter that violates conventional energy conditions, they can still yield a positive active gravitational mass [53,54]. The active gravitational mass function $M(r)$, enclosed within a radial distance r, can be evaluated by integrating the energy density over the wormhole volume as follows:

$$M_{act.} = 4\pi \int_{r_0}^{r} \rho(r)\, r^2\, dr, \tag{66}$$

By considering Eqs. (34) and (66), we get active mass of conformal wormhole as follows:

$$M_{act.} = \left[\frac{-8\pi\left(-r k_2^2 \beta + k_3 \lambda\, r^{-\frac{3\beta}{2\lambda - \beta}}\right)}{k_2^2 \lambda(\lambda + \beta)} \right]_{r_0}^{r}. \tag{67}$$

The active gravitational mass of conformal wormhole is illustrated in Fig. 8. The monotonic increase and positivity of M_{eff} indicate a net attractive nature despite the presence of phantom matter, supporting the physical plausibility of the wormhole configuration. This behavior emphasizes that, although supported by exotic matter, the wormhole retains a positive active gravitational mass, thereby rendering its gravitational signature consistent with that of standard matter distributions.

4.7. Total gravitational energy

The current section, we evaluate the total gravitational energy E_g of the wormhole configuration by employing the approach introduced by Lynden-Bell et al. [55], and later extended by Nandi et al. [56]. This method allows for a meaningful decomposition of the system's total energy content into gravitational and mechanical components. More precisely, gravitational energy corresponds to the residual part of the total energy Mc^2 once the mechanical energy E_M has been excluded, and is expressed as:

$$E_g = Mc^2 - E_M. \tag{68}$$

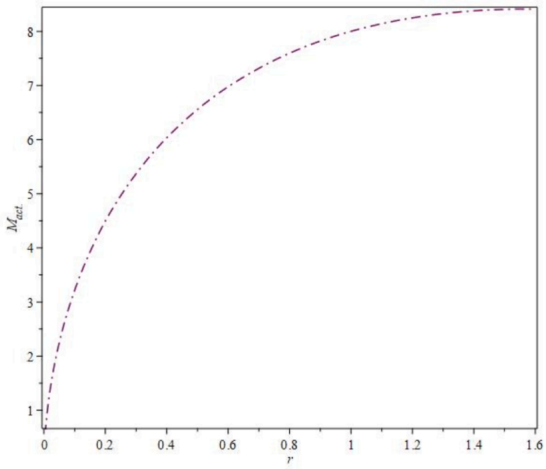

Fig. 8. The evolution of active gravitational mass for conformal wormhole ($k_2 = 1, k_3 = -1, \beta = -\frac{\pi}{2}, \lambda = \pi$ and $r_0 = 1$).

Table 1
The calculated values of E_g for different upper limits R.

Upper Limit R	Value of E_g
1.1	0.48673124
1.2	0.47221011
1.3	0.46457379
1.4	0.46048632
1.5	0.45861426
1.57	0.45823671

Here, the total energy Mc^2 and mechanical energy E_M are computed through the following integrals:

$$Mc^2 = \frac{1}{2}\int_{r_0^+}^{R} \rho(r)\, r^2\, dr + \frac{r_0}{2}, \quad E_M = \frac{1}{2}\int_{r_0^+}^{R} \sqrt{g_{rr}}\, \rho(r)\, r^2\, dr, \tag{69}$$

where $g_{rr} = \left(1 - \frac{S(r)}{r}\right)^{-1}$ is the radial component of the metric tensor. These definitions enable the gravitational energy to be rewritten as:

$$E_g = \frac{1}{2}\int_{r_0^+}^{R} \left[1 - \sqrt{g_{rr}}\right] \rho(r)\, r^2\, dr + \frac{r_0}{2}. \tag{70}$$

Owing to the mathematical complexity of the metric component g_{rr} and the energy density function $\rho(r)$, it is not feasible to obtain a closed form analytical expression for the integral. Therefore, the total gravitational energy E_g is computed numerically. For this purpose, the lower integration limit is fixed at $r_0^+ = 1.05$, while various upper limits are considered. The corresponding numerical values of E_g are summarized in Table 1.

An important result arising from our analysis is that the total gravitational energy E_g remains positive throughout the wormhole configuration. This indicates that, despite the presence of exotic matter violating the null energy condition, the overall gravitational energy content of the system does not exhibit any unphysical behavior. The positivity of E_g suggests that the wormhole spacetime exhibits a net attractive influence and remains gravitationally bound. Such behavior is highlights the influence of the matter-curvature coupling in the framework of $f(R, L_m, T)$ gravity.

5. Conclusion

In this work, we have constructed traversable wormhole solutions in $f(R, L_m, T)$ gravity, assuming that the spacetime admits conformal symmetry. The matter source is modeled using a phantom energy equation of state, and exact analytical expressions for the metric components, energy density, and pressure terms are attained. The viability of the resulting wormhole solution is then examined under a set of physically motivated conditions, supported by detailed geometric and physical analyses.

The results and interpretations related to each key aspect of the wormhole configuration are summarized below:

- The 2D and 3D embedding diagrams are successfully constructed based on the derived shape function. These diagrams confirm that the wormhole structure is smooth, symmetric, and flares outward near the throat, satisfying the geometric visualization of a traversable wormhole.

- The proper distance $l(r)$ between the throat and any point outside was shown to be greater than the corresponding coordinate distance, as expected. Also, the $l(r)$ function is greater than the $z(r)$ function for the conformal wormhole. The function $l(r)$ decreases monotonically toward the throat and diverges symmetrically away from it, confirming the wormhole's traversability.
- While the null and weak energy conditions are violated due to the use of phantom energy, the violations are slower and spatially localized near the throat. The tangential pressure $p_t(r)$ changes sign across the throat, offering a potential stabilizing mechanism for the geometry.
- The equilibrium condition was analyzed by decomposing the forces acting on the fluid into hydrostatic, gravitational, anisotropic, and additional coupling-induced terms. The balance among these forces was numerically verified, demonstrating that the wormhole remains in a stable hydrostatic equilibrium.
- The volume integral I_V, which measures the total amount of energy condition-violating matter, is evaluated analytically and shown to approach zero as the integration limit approaches the throat. This result indicates that the wormhole can, in principle, be supported by a vanishingly small amount of exotic matter.
- Despite being supported by exotic matter, the wormhole exhibits a positive active gravitational mass throughout its structure. This suggests that its gravitational influence would exhibits that of ordinary matter when observed from afar.
- The total gravitational energy E_g is calculated numerically and found to be positive for all tested configurations. This is a significant result, indicating that the wormhole is dynamically bound and does not introduce unphysical behavior despite its exotic matter content.
- The wormhole's lack of horizons and its positive active gravitational mass make it a viable candidate for compact gravitational lensing, potentially yielding observational features such as multiple or shifted Einstein rings not typically expected from black hole systems [57,58]. Such lensing signatures could, in principle, serve as observational discriminants between wormholes and standard compact objects in future astrophysical surveys.

These findings collectively demonstrate that $f(R, L_m, T)$ gravity allows for the existence of traversable wormholes that are not only analytically tractable but also physically meaningful. The ability to obtain stable solutions with minimal exotic matter strengthens the theoretical foundation for wormhole models in modified gravity. While we have adopted a linear $f(R, L_m, T)$ model to obtain analytic wormhole solutions under conformal symmetry, it is worth noting that non-linear extensions could lead to richer phenomenology. A detailed exploration of these cases could be studied for future work.

Data availability

No data was used for the research described in the article.

Declaration of competing interest

The authors declare that they have no known competing financial interests or personal relationships that could have appeared to influence the work reported in this paper.

References

[1] K.L. Duggal, Curvature inheritance symmetry in Riemannian spaces with applications to fluid space times, J. Math. Phys. 33 (9) (1992) 2989–2997.
[2] L. Herrera, J. Ponce de Leon, Isotropic and anisotropic charged spheres admitting a one-parameter group of conformal motions, J. Math. Phys.(NY);(United States) 26 (9) (1985).
[3] M.S. Morris, K.S. Thorne, Wormholes in spacetime and their use for interstellar travel: a tool for teaching general relativity, Am. J. Phys. 56 (1988) 395–412.
[4] D. Hochberg, M. Visser, The quantum physics of traversable wormholes, Phys. Rev. D 58 (1998) 044021. https://doi.org/10.1103/PhysRevD.58.044021
[5] R. Garattini, Self-sustained traversable wormholes?, Class. Quantum Grav. 22 (2005) 1105–1118. https://doi.org/10.1088/0264-9381/22/6/011
[6] F.S.N. Lobo, Exotic solutions in general relativity: traversable wormholes and 'warp drive' spacetimes, Class. Quantum Grav. 21 (2004) 2195–2202. https://doi.org/10.1088/0264-9381/21/9/001
[7] P.K.F. Kuhfittig, A wormhole with a special shape function, Am. J. Phys. 67 (2) (1999) 125–126.
[8] C. Armendariz-Picon, On a class of stable, traversable Lorentzian wormholes in classical general relativity, Phys. Rev. D 65 (10) (2002) 104010.
[9] P. Gao, D.L. Jafferis, A.C. Wall, Traversable wormholes via a double trace deformation, J. High Energy Phys. 2017 (12) (2017) 1–25.
[10] E. Caceres, A. Kundu, A.K. Patra, S. Shashi, A killing vector treatment of multiboundary wormholes, J. High Energy Phys. 2020 (2) (2020) 1–32.
[11] T. Harko, F.S.N. Lobo, M.K. Mak, S.V. Sushkov, Modified-gravity wormholes without exotic matter, Phys. Rev. D 87 (6) (2013) 067504. https://doi.org/10.1103/PhysRevD.87.067504
[12] M. Zubair, G. Mustafa, S. Waheed, Exact wormhole solutions without exotic matter in $f(R,T)$ gravity, Int. J. Geom. Methods Mod. Phys. 16 (06) (2019) 1950046. https://doi.org/10.1142/S0219887819500464
[13] J.L. Rosa, P.M. Kull, Non-exotic traversable wormhole solutions in linear $f(R,T)$ gravity, Euro. Phys. J. C 82 (10) (2022) 941. https://doi.org/10.1140/epjc/s10052-022-11135-w
[14] J.L. Rosa, J.P.S. Lemos, F.S.N. Lobo, Wormholes in generalized hybrid metric-Palatini gravity obeying the matter null energy condition everywhere, Phys. Rev. D-Particles, Fields, Gravit., and Cosmol. 98 (6) (2018) 064054.
[15] F.R. Klinkhamer, Defect wormhole: A traversable wormhole without exotic matter, Acta Phys. Pol. B 54 (2023) 5-A3.
[16] D.g. Taser, M.U. Doğru, E. Eraslan, H. Aydın, Conformal wormholes in $f(R, L_m)$ theory, Phys. Scr. 99 (7) (2024) 075049.
[17] A. Banerjee, K.N. Singh, M.K. Jasim, F. Rahaman, Conformally symmetric traversable wormholes in f (R, T) gravity, Ann. Phys. 422 (2020) 168295.
[18] H. Wu, Traversable phantom wormholes via conformal symmetry in f (R, φ, χ) gravity, Int. J. Geom. Methods Mod. Phys. 18 (13) (2021) 2150210.
[19] M. Jan, A. Ashraf, A. Basit, A. Caliskan, E. Güdekli, Traversable wormhole in f (Q) gravity using conformal symmetry, Symmetry 15 (4) (2023) 859.
[20] M. Tayde, Z. Hassan, P.K. Sahoo, Conformally symmetric wormhole solutions supported by non-commutative geometries in the context of f (Q, T) gravity, Chin. J. Phys. 89 (2024) 195–209.
[21] A.G. Riess, A.V. Filippenko, P. Challis, A. Clocchiatti, A. Diercks, P.M. Garnavich, R.L. Gilliland, C.J. Hogan, S. Jha, R.P. Kirshner, et al., Observational evidence from supernovae for an accelerating universe and a cosmological constant, Astron. J. 116 (1998) 1009. https://doi.org/10.1086/300499

[22] S. Perlmutter, G. Aldering, G. Goldhaber, R.A. Knop, P. Nugent, P.G. Castro, S. Deustua, S. Fabbro, A. Goobar, D.E. Groom, et al., Measurements of Ω and Λ from 42 high-redshift supernovae, Astrophys. J. 517 (2) (1999) 565.

[23] S. Nojiri, S.D. Odintsov, Unified cosmic history in modified gravity: from F(R) theory to Lorentz non-invariant models, Phys. Rep. 505 (2011) 59–144. https://doi.org/10.1016/j.physrep.2011.04.001

[24] T. Clifton, P.G. Ferreira, A. Padilla, C. Skordis, Modified gravity and cosmology, Phys. Rep. 513 (2012) 1–189. https://doi.org/10.1016/j.physrep.2012.01.001

[25] Z. Haghani, T. Harko, Generalizing the coupling between geometry and matter: $f(R, L_m, T)$ gravity, The Euro. Phys. J. C 81 (7) (2021) 615.

[26] T. Harko, F.S.N. Lobo, Generalized curvature-matter couplings in modified gravity, Galaxies 2 (3) (2014) 410–465. https://doi.org/10.3390/galaxies2030410

[27] S.S. Mishra, J.A.S. Fortunato, P.H.R.S. Moraes, P.K. Sahoo, Cosmography of $f(R, L, T)$ gravity, Phys. Dark Universe 48 (2025) 101831. https://doi.org/10.1016/j.dark.2025.101831

[28] M. Zubair, S. Waheed, Q. Muneer, M. Ahmad, Thermodynamics and perturbative analysis of some newly developed $f(R, L_m, T)$ theories, Fortschr. Phys. 71 (8-9) (2023) 2300018. https://doi.org/10.1002/prop.202300018

[29] S. Arora, P. Moraes, P.K. Sahoo, Energy conditions in the f (R, L, T) theory of gravity, Euro. Phys. J. Plus 139 (6) (2024) 1–7.

[30] D.C. Maurya, Late-time accelerating cosmological models in $f(R, L_m, T)$ gravity with observational constraints, Phys. Dark Universe 46 (2024) 101722. https://doi.org/10.1016/j.dark.2024.101722

[31] J.S. Gonçalves, A.F. Santos, On causality and its violation in $f(R, L_m, T)$ gravity, Nucl. Phys. B 1010 (2025) 116751. https://doi.org/10.1016/j.nuclphysb.2024.116751

[32] P.H.R.S. Moraes, A.S. Agrawal, B. Mishra, Wormholes in the $f(R, L, T)$ theory of gravity, Phys. Lett. B 855 (2024) 138818. https://doi.org/10.1016/j.physletb.2024.138818

[33] A. Errehymy, Y. Khedif, M. Daoud, K. Myrzakulov, A.-H. Abdel-Aty, K.S. Nisar, Einstein clusters as dark matter fluid-like models for constructing new wormhole solutions in $f(R, L_m, T)$ gravity, J. High Energy Astrophys. 47 (2025) 100370. https://doi.org/10.1016/j.jheap.2025.100370

[34] T. Naseer, M. Sharif, M. Faiza, W. Albalawi, A.H. Abdel-Aty, Astrophysical signatures of traversable wormholes in modified gravity: implications of different equations of state and complexity analysis, Phys. Dark Universe 48 (2025) 101890. https://doi.org/10.1016/j.dark.2025.101890

[35] M. Tayde, P.K. Sahoo, Role of EoS in wormhole through $f(R, L_m, T)$ gravity, Phys. Dark Universe 49 (2025) 101971. https://doi.org/10.1016/j.dark.2025.101971

[36] M. Tayde, D. Mohanty, P.K. Sahoo, A study of wormhole solution using MIT bag parameter in the framework of $f(R, L_m, T)$ gravity, Phys. Dark Universe 48 (2025) 101937. https://doi.org/10.1016/j.dark.2025.101937

[37] C.E. Mota, J.M.Z. Pretel, C.O.V. Flores, Neutron stars in f (R, L m, T) gravity, Euro. Phys. J. C 84 (7) (2024) 673.

[38] P.K.F. Kuhfittig, Gravitational lensing of wormholes in the galactic halo region, Euro. Phys. J. C 74 (3) (2014) 2818.

[39] D. Mohanty, M. Tayde, P.K. Sahoo, Non-commutative gravastar configuration in $f(R, L_m, T)$ gravity, Nucl. Phys. B 1016 (2025) 116914.

[40] L. Herrera, J. Jimenez, L. Leal, J. Ponce de Leon, M. Esculpi, V. Galina, Anisotropic fluids and conformal motions in general relativity, J. Math. Phys. 25 (11) (1984) 3274–3278.

[41] R. Maartens, M.S. Maharaj, Conformally symmetric static fluid spheres, J. Math. Phys. 31 (1) (1990) 151–155.

[42] C.G. Böhmer, T. Harko, F.S.N. Lobo, Wormhole geometries with conformal motions, Classical Quantum Gravity 25 (7) (2008) 075016.

[43] K.P. Das, U. Debnath, Possible existence of traversable wormhole in Finsler–Randers geometry, Euro. Phys. J. C 83 (9) (2023) 821.

[44] F.S.N. Lobo, Wormholes, Warp Drives and Energy Conditions, 189, Springer, 2017.

[45] B. Ghosh, S. Mitra, Wormhole solutions in f (R) gravity theory for Chaplygin gas scenario, Intern. J. Modern Phys. A 36 (18) (2021) 2150119.

[46] A. Raychaudhuri, Relativistic cosmology. I, Phys. Rev. 98 (4) (1955) 1123.

[47] J.R. Oppenheimer, G.M. Volkoff, On massive neutron cores, Phys. Rev. 55 (4) (1939) 374.

[48] P.K.F. Kuhfittig, A note on the stability of Morris-Thorne wormholes, arXivpreprintarXiv:2009.11179 (2020).

[49] M. Visser, S. Kar, N. Dadhich, Traversable wormholes with arbitrarily small energy condition violations, Phys. Rev. Lett. 90 (20) (2003) 201102.

[50] C.G. Böhmer, T. Harko, F.S.N. Lobo, Conformally symmetric traversable wormholes, Phys. Rev. D-Particles, Fields, Gravit., and Cosmol. 76 (8) (2007) 084014.

[51] F.S.N. Lobo, Phantom energy traversable wormholes, Phys. Rev. D-Particles, Fields, Gravit., and Cosmol. 71 (8) (2005) 084011.

[52] F.S.N. Lobo, Stability of phantom wormholes, Phys. Rev. D-Particles, Fields, Gravit., and Cosmol. 71 (12) (2005) 124022.

[53] F. Rahaman, P. Kuhfittig, S. Ray, N. Islam, Possible existence of wormholes in the galactic halo region, Euro. Phys. J. C 74 (2) (2014) 2750.

[54] M.M. Rizwan, Z. Hassan, P.K. Sahoo, A. Övgün, Influence of GUP corrected Casimir energy on zero tidal force wormholes in modified teleparallel gravity with matter coupling, Euro. Phys. J. C 84 (11) (2024) 1132.

[55] D. Lynden-Bell, J. Katz, J. Bičák, Energy and angular momentum densities of stationary gravitational fields, Phys. Rev. D-Particles, Fields, Gravit., and Cosmol. 75 (2) (2007) 024040.

[56] K.K. Nandi, Y.Z. Zhang, R.G. Cai, A. Panchenko, Energetics in condensate star and wormholes, Phys. Rev. D-Particles, Fields, Gravit., and Cosmol. 79 (2) (2009) 024011.

[57] R. Shaikh, P. Banerjee, S. Paul, T. Sarkar, Strong gravitational lensing by wormholes, J. Cosmol. Astropart. Phys. 2019 (07) (2019) 028.

[58] T.K. Dey, S. Surajit, Gravitational lensing by wormholes, Mod. Phys. Lett. A 23 (13) (2008) 953–962.